

Stacked Convolutional Neural Network for Diagnosis of COVID-19 Disease from X-ray Images

Mahesh Gour ^{1*}, Sweta Jain ²

**corresponding author: maheshgour0704@gmail.com*

^{1,2} *Maulana Azad National Institute of Technology, Bhopal, MP, India 462003*

Abstract

Automatic and rapid screening of COVID-19 from the chest X-ray images has become an urgent need in this pandemic situation of SARS-CoV-2 worldwide in 2020. However, accurate and reliable screening of patients is a massive challenge due to the discrepancy between COVID-19 and other viral pneumonia in X-ray images. In this paper, we design a new stacked convolutional neural network model for the automatic diagnosis of COVID-19 disease from the chest X-ray images. We obtain different sub-models from the VGG19 and developed a 30-layered CNN model (named as CovNet30) during the training, and obtained sub-models are stacked together using logistic regression. The proposed CNN model combines the discriminating power of the different CNN's sub-models and classifies chest X-ray images into COVID-19, Normal, and Pneumonia classes. In addition, we generate X-ray images dataset referred to as COVID19CXr, which includes 2764 chest x-ray images of 1768 patients from the three publicly available data repositories. The proposed stacked CNN achieves an accuracy of 92.74%, the sensitivity of 93.33%, PPV of 92.13%, and F1-score of 0.93 for the classification of X-ray images. Our proposed approach shows its superiority over the existing methods for the diagnosis of the COVID-19 from the X-ray images.

Keywords: COVID-19, automatic screening, stacked generalization, ensemble technique, deep learning, logistic regression, chest X-ray images.

1. INTRODUCTION

The Novel coronavirus disease 2019 (COVID-19) pandemic has put the livelihoods and health of the massive population in a critical position. It has led to the disturbance throughout the public life of the world population. The severe acute respiratory syndrome coronavirus 2 (SARSCoV-2) belongs to the family of Coronavirus, which get transmitted in the people based on the infection in the form of direct contact or fomites. The primary symptoms of coronavirus infection are fever, cough and fatigue. In several cases coronavirus cause severe respiratory problems like Pneumonia, lung disorders and kidney malfunction. The virus has serious consequences as its serial interval is 5 to 7.5 days, and the rate of reproduction is 2 to 3 [1] people. The coronavirus infection can incite SARS (Severe Acute Respiratory Syndrome), which might unfold serious health impacts.

It is estimated that many people are healthy carriers of a virus, and they are the reason for about 5% to 10% of acute respiratory infections [2]. A critical step to fight against the COVID-19 is to identify the infected people so that they get immediate treatment and isolate them to control the multiplying of the spread of the infection.

The COVID-19 panic has increased due to the unavailability of fast and accurate diagnosis systems to test the infected people. According to the World Health Organization (WHO), the diagnosis of COVID-19 cases must be confirmed by molecular assay, such as the reverse transcription polymerase chain reaction (RT-PCR) pathological test using throat swab samples [3]. While RT-PCR has become a standard tool for confirmation of COVID-19, but it is a very time consuming, laborious, and manual process, and there is a limitation of availability of diagnostic kits and sample collection. The availability of COVID-19 testing kits is limited as compared to the increasing amount of infected people; hence there is a need to rely on different diagnosis methodologies.

The coronavirus targets the epithelial cells that affect patients respiratory tract, which can be analyzed by the radiological images of a patients lungs.

Some early studies also show that patients present anomalies in chest x-ray images, which are the typical characteristics of COVID-19 infected patients [4, 5]. Hence, the development of the computer-aided diagnosis system for the automatic analysis of radiological images can be very helpful in identifying infected patients at a faster rate. Some the advantage of the using X-ray images for COVID-19 screening as follows:

- Enable fast screening and rapid triaging of patients suspected of COVID-19.
- Making use of readily available and accessible radiological images.
- Portable and easy to setup, these systems can be setup in the isolation room, which significantly minimizes the risk of transmission.

Recent advancements in deep learning specifically in Convolution Neural Network (CNN) motivated us to develop a highly reliable computer-aided diagnosis (CAD) systems for the rapid detection of the COVID-19 using chest X-ray images. It will enable and enhance the automation in the screening phase, which is the crucial part of the COVID-19 pandemic. In this study, we design a new stacked convolutional neural network for automatic diagnosis of COVID-19 disease from the chest X-ray images. To train the proposed model, we generated chest X-ray images dataset, with the combination and modification of three publicly available datasets [6, 7, 8], which we will refer to as COVID19CXr.

The organization of this paper as follows: Section 2 presents the related work. Section 3 describes the proposed stacked CNN model for the classification of COVID-19, Normal, and Pneumonia X-ray images. Section 4 describes the COVID19CXr dataset generation process and details the experimental results, performance comparison. Finally, the conclusion is drawn in Section 5.

2. RELATED WORK

Over the past 40 years, many computer-aided systems have been developed for the diagnosis of lung disease [9] and achieved promising results for automatic

detecting lung abnormality from the radiological images [10, 11, 12].

Recently, automatic CAD of COVID-19 using radiological images has drawn a lot of attention of researchers and as a result several approaches have been introduced in literature. They have published a series of research articles [13, 14] demonstrating the CAD systems for the detection of COVID-19 using radiological images. Butt et al. [15] have studied various CNN models technically and proposed a model with the combination of 2D and 3D CNN models for the classification of the CT images into COVID-19, Influenza viral pneumonia, or no-infection. Their approach achieved a sensitivity of 98.2 % and specificity of 92.2 %. Ardakani et al. [16] have presented the application of deep learning in COVID-19 detection using CT images. Authors tested ten pre-trained CNN models namely AlexNet, MobileNet-V2 VGG-16, VGG-19, ResNet-18, ResNet-50, ResNet-101, SqueezeNet, GoogleNet, and Xception. Their experiment results showed that ResNet101 performed best with area under the curve (AUC) of 0.99 over 1020 CT images of 194 patients.

Similarly, Narin et al. [17] have applied ResNet50, InceptionV3 and Inception-ResNetV2 using transfer learning for classification of the X-ray images into normal and COVID-19 class. This method achieved good performance with an accuracy of 98 % with ResNet50. However, the number of X-ray images are only 100 and the number of images was very less. Wang et al. [18] have proposed an open-source COVID-Net model based on the projection-expansion-projection design pattern for COVID-19 cases detection from the X-ray images. In this study, the authors reported an accuracy of 92.6 %. Oh et al. [19] have proposed patch-based CNN approach, to train ResNet18 model using image patches that have been extracted from the chest x-ray images. For decision making, they used the majority voting strategy, which resulted in an accuracy of 88.9 %.

An objected detection based DarkCovidNet model has been proposed by Ozturk et al. [20] for automatic detection of COVID-19 cases from the X-ray images. They have reported accuracy of 98.08 % for binary classification of X-ray images into COVID-19 and no-findings, and also this approach has achieves an accuracy of 87.02 % for multi-class classification of X-ray images

into COVID-19, no-findings and pneumonia. Pereira et al. [21] have proposed a hierarchical classification approach, in which they extracted deep features by InceptionV3 and tested texture descriptors. They investigated early and late fusion techniques for combining the strength of descriptor and classifiers. Their hierarchical classification approach achieved F1-Score of 0.89 for the COVID-19 identification in the X-ray images.

Attention-based deep 3D multiple instance learning approach has been proposed by the Han et al. [22] for automatic screening of COVID-19 from the CT images. Their algorithm achieved an accuracy of 97.9%. Wang et al. [23] developed a weakly supervised deep learning framework, in which lung region was segmented by UNet from the CT images and 3D deep neural network is applied on the segmented region for predicting probability of COVID-19 infections. Authors reported an accuracy of 90.10%.

Ucar et al. [24] proposed a SqueezeNet CNN model with Bayesian optimization for diagnosis of the COVID-19 from X-ray images. They reported an accuracy of 98.26 %. Afshar et al. [25] developed a capsule network-based framework for the classification of the X-ray images into Normal, bacterial, Non-COVID, and COVID-19 cases. The authors reported an accuracy of 95.7 % and a sensitivity of 90 %. Sethy et al. [26] extracted deep features of X-ray images from the pre-trained CNN, and support vector machine (SVM) has been applied on the extracted feature to classify x-ray images. The authors achieved an accuracy of 95.38% using ResNet50 with the SVM classifier.

3. METHODOLOGY

The Convolution Neural Network is the driving concept of deep learning algorithms in computer vision, which led to outstanding performance in most of the pattern recognition tasks such as image classification [27, 28, 29], object localization, segmentation and detection [30, 31, 32]. It has also shown its superiority in the medical image analysis for image classification, and segmentation problem [33, 34, 35, 36], especially in lung-related diseases such as lung nodule

detection [37], pneumonia detection [38], and pulmonary tuberculosis [39]. CNN automatically learns a low to the high level of useful feature representations and integrates feature extraction and classification stages in a single pipeline, which is trainable in an end-to-end manner without requiring any manual design and expert human intervention.

In this work, we have developed a deep learning-based stacked convolutional neural network for the rapid screening of COVID-19 patients using X-ray images. The proposed COVID-19 detection method includes three modules as shown in the Figure 1. In the first module, a new 30-layered CNN model is built and trained on the chest X-ray images from scratch, which will be referred to as CovNet30 (**Covid-19 Network of 30-layers**). In the second module, a pre-trained VGG19 model [27] is fine-tuned on X-ray images for the diagnosis of COVID-19 disease. Finally, in the last module, five CNN's sub-models are obtained, during the training of CovNet30 and VGG19 models. The output of CNN's sub-models are stacked together by applying logistic regression [40]

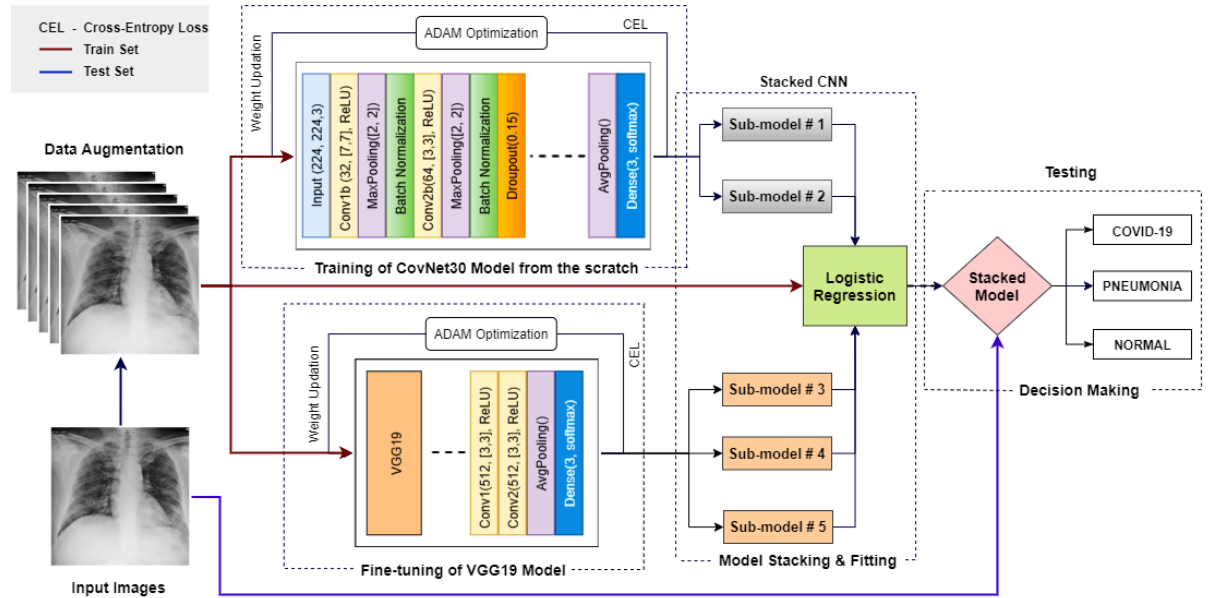


Figure 1: Block diagram of proposed Stacked CNN model

for building a new final CNN model for diagnosis of COVID-19 disease from X-ray images. A detailed description of the proposed approach is given in the following section:

3.1. CovNet30 Architecture and Training

The CovNet30 is a task-specific, 30-layered convolutional neural network for X-ray images classification. It learns the non-linear, discriminative features directly from the chest X-ray images at multiple levels of abstraction. A detailed layer configuration of the CovNet30 network is shown in Table 1. CovNet30 is sequential network, in which Convolutional layer with ReLU activation, pooling layer, Batch Normalization layer and dropout layer are added repetitively. Every layer of CovNet30 produce a volume of activation to the next layer through a differentiable function. Description of layers are given as follows:

- Convolution Layer extracts features from the input volume by performing convolution operation. In the convolution operation, the dot product is computed between the kernels and connected local regions of the input volume of activation.
- ReLU activation function is an elementwise activation function. If x is input of ReLU then it produce $\max(0, x)$ (non-negative value) in the output.
- Pooling layer down sampling feature maps and reduces the computation in the network.
- Batch Normalization layer speed up the learning process and improves network stability by minimizing the internal covariate shift.
- Dropout is a regularization method, which prevents the network from the overfitting by dropping out units in the network.

CovNet30 has been trained on the X-ray images in a supervised manner. Cross-entropy loss function is used to calculate the training error and which

Table 1: Detailed layer configuration of CovNet30 network

Layer Name	Type	Kernal Size	Output	Parameters
conv2D_1	Convolutional + ReLU	7×7	$218 \times 218 \times 32$	4736
max_pooling_1	Max Pooling	2×2	$109 \times 109 \times 32$	0
batchNo.1	Batch Normalization	-	$109 \times 109 \times 32$	128
conv2D_2	Convolutional + ReLU	5×5	$105 \times 105 \times 64$	51264
max_pooling_2	Max Pooling	2×2	$52 \times 52 \times 64$	0
batchNo.2	Batch Normalization	-	$52 \times 52 \times 64$	256
dropout.1	Dropout	-	$52 \times 52 \times 64$	0
conv2D_3	Convolutional + ReLU	3×3	$50 \times 50 \times 128$	73856
max_pooling_3	Max Pooling	2×2	$25 \times 25 \times 128$	0
batchNo.3	Batch Normalization	-	$25 \times 25 \times 128$	512
dropout.2	Dropout	-	$25 \times 25 \times 128$	0
conv2D_4	Convolutional + ReLU	3×3	$23 \times 23 \times 128$	147584
max_pooling_4	Max Pooling	2×2	$11 \times 11 \times 128$	0
batchNo.4	Batch Normalization	-	$11 \times 11 \times 128$	512
dropout.3	Dropout	-	$11 \times 11 \times 128$	0
conv2D_5	Convolutional + ReLU	3×3	$9 \times 9 \times 256$	295168
batchNo.5	Batch Normalization	-	$9 \times 9 \times 256$	1024
dropout.4	Dropout	-	$9 \times 9 \times 256$	0
conv2D_6	Convolutional + ReLU	3×3	$7 \times 7 \times 256$	590080
batchNo.6	Batch Normalization	-	$7 \times 7 \times 256$	1024
dropout.5	Dropout	-	$7 \times 7 \times 256$	0
conv2D_7	Convolutional + ReLU	3×3	$5 \times 5 \times 512$	1180160
batchNo.7	Batch Normalization	-	$5 \times 5 \times 512$	2048
dropout.6	Dropout	-	$5 \times 5 \times 512$	0
conv2D_8	Convolutional + ReLU	3×3	$3 \times 3 \times 512$	2359808
batchNo.8	Batch Normalization	-	$3 \times 3 \times 512$	2048
dropout.7	Dropout	-	$3 \times 3 \times 512$	0
globAvgPooling	Global AvgPooling	-	512	0
FC.1	Fully Connected + ReLU	-	1000	513000
FC.2	Fully Connected + Softmax	-	3	3003

is minimize using the ADAM optimizer [41]. Cross-entropy loss function is mathematical represented in equation (1).

$$J(T, P) = - \sum_{i=1}^C t_i \log(p_i) \quad (1)$$

Where t_i and p_i are the target value and predicted probability for each class i in C .

In the experiment, the values of hyper-parameter are set as follows: learning rate to 0.001, the batch size to 16, and dropout probability to 0.15. we experimentally find that these are the best suitable values of hyper-parameters for network training.

3.2. Fine-Tuning of VGG19

The VGG19 is a pre-trained network that is trained on the ImageNet dataset, which achieved state-of-the-art performance on ILSVRC Challenge 2014. It also achieves outstanding performance on the other image recognition datasets. Hence, we have also used VGG19 along with CovNet30 for generating sub-models.

To fine-tune the VGG19 on X-ray images, the top layers (Fully-connected layer, and Softmax layer) of the VGG19 network are removed. We added new layers such as two Convolutional layers with ReLU activation, a Global Average Pooling layer, a Fully-connected layer, and a Softmax layer, at the top of the VGG19 network. Hyper parameters for the fine-tuning of VGG19 are same as the CovNet30.

3.3. Stacked Convolutional Neural network

Stacked generalization [42] is an ensemble approach in which a new model learns how to incorporate the best predictions of multiple existing models. The proposed approach hypothesized that different CNN's sub-models learn non-linear discriminative features and semantic image representation from the images at different levels. Thus a stacked ensemble CNN model will be generalized and highly accurate. This section describes the proposed stacked convolutional neural network.

The pseudo-code of sub-models generation process is given in Algorithm 1. In this process the Covid19CXr dataset is divided in the train set, validation set and test set. The CovNet30 and VGG19 are trained on chest x-ray images of the training set for the 1530 iterations and 2121, respectively. During training

Algorithm 1 Sub-model Generation process

Input: X-ray images of the chest

Output: sub-models

- 1: Divide Covid19CXr dataset into training set, validation set and test set.
 - 2: Apply data augmentation on train set.
 - 3: Train CovNet30 and VGG19, and generate sub-models:
Initialisation : class_weight = [0:30, 1:1, 1:1]
 - 4: **for** $i = 1$ to N **do**
 - 5: Train(CovNet30, train_img, img_label, class_weight)
 - 6: **if** ($i == l1$) **then**
 - 7: sub-model#1 = save(CovNet30)
 - 8: **end if**
 - 9: **end for**
 - 10: sub-model#2 = save(CovNet30)
 - 11: **for** $i = 1$ to M **do**
 - 12: Train(VGG19, train_img, img_label, class_weight)
 - 13: **if** ($i == l1$) **then**
 - 14: sub-model#3 = save(VGG19)
 - 15: **else**
 - 16: **if** ($i == l2$) **then**
 - 17: sub-model#4 = save(VGG19)
 - 18: **end if**
 - 19: **end if**
 - 20: **end for**
 - 21: sub-model#5 = save(VGG19)
 - 22: **return** *sub-models*
-

of CovNet30, we have extracted the first *sub-model#1* after 765 iterations and second *sub-model#2* after completion of the training. Similarly, during fine-tuning of VGG19, we have extracted *sub-model#3* after 707 iterations, *sub-model#4* after 1414 iterations, and *sub-model#5* at last.

To deal with the class imbalance problem, we have assigned class weights while training of the networks. In this process, class weight in ratio of 30:1:1 is assigned to COVID-19, Pneumonia, and Normal class, respectively.

The performance of the sub-models varies across complex CAD systems, and it is reasonable to combine the strengths of sub-models which might result in increased overall accuracy. Hence, we combined the sub-models output by logistic regression [40] to build a highly accurate and reliable generalized model. The pseudo-code of the process of creating stacked CNN is represented in Algorithm 2.

Algorithm 2 Stacked Convolutional Neural network and X-ray image Classification

Input: Validation set, test set, and sub-models

Output: Classification results

- 1: Sub-Models Stacking:
 - 2: **for** $i = 1$ to $length(validation\ set)$ **do**
 - 3: **for** $j = 1$ to 5 **do**
 - 4: $[P1_{ji}, P2_{ji}, P3_{ji}] = sub-model\#(j).predict(validation_img[i])$
 - 5: **end for**
 - 6: $P = concatenation([P1_{ji}, P2_{ji}, P3_{ji}])$
 - 7: **end for**
 - 8: Fit logistic regression on feature vector P
 - 9: $stacked_model = fit.regression(P, validation_label)$
 - 10: Classifies X-ray image
 - 11: $pred_label = classify(stacked_model, test_img)$
 - 12: **return** $pred_label$
-

The hypothesis representation of logistic regression model is as shown below:

$$H_{\theta}^i(x) = g(\theta^T x) \quad (2)$$

$$\text{where } g(z) = \frac{1}{1 + e^{-z}} \quad (3)$$

$$\text{hence } H_{\theta}^i(x) = \frac{1}{1 + e^{-\theta^T x}} \quad (4)$$

Where $H_{\theta}^i(x)$ is estimated probability $p(y = i/x; \theta)$ for each class i (where $i \in \{0 : COVID - 19, 1 : Normal, 2 : Pneumonia\}$) of a image x .

Next, we train a logistic regression model $H_{\theta}^i(x)$ using a one-vs-rest scheme [43] for each class i . For its training, we prepared dataset by providing X-ray images from the validation set to each of the sub-models and collects predictions.

In this case, every sub-model j predicts three probabilities ($P1_{ji}$, $P2_{ji}$, $P3_{ji}$) for each X-ray image i of that a given image i belongs to each of the COVID-19, Normal, and Pneumonia classes. Let's say M X-ray images in the validation set, and we concatenate the output probabilities of these five sub-models that become our feature vector $P_{M \times 15}$ for the training of the logistic regression model. After training of the stacked model, on new input image x from the test set, to make a prediction, pick the class i that maximizes $max_i(H_{\theta}^i(x))$.

4. EXPERIMENTS

This section presents the details of the dataset, evaluation metrics, experiments results and performance comparison.

4.1. Covid19CXr Dataset Generation

In order to train and evaluate the performance of the proposed model, we generated X-ray images dataset, with the combination and modification of three publicly available datasets [6, 7, 8], which are referred as COVID19CXr. The COVID19CXr includes 2764 chest X-ray images of 1768 patients. Out of 2764 images, 270 images of 170 patients belong to a COVID-19 class, 1139 images of

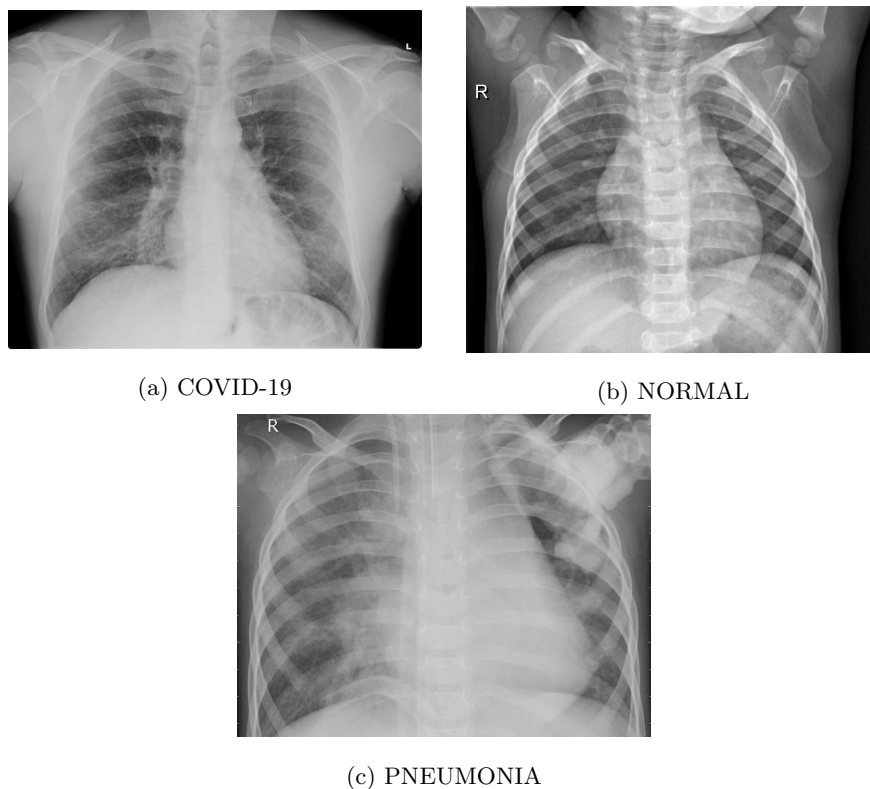


Figure 2: Samples of X-ray images of Chest from the database; where image in (a) COVID-19, (b) NORMAL, (c) PEUMONIA

1015 patients belong to Normal class and 1355 images of 583 patients belong to a Pneumonia class. COVID-19 images are obtained from the two publicly available repositories: 1) “*Figure-1 COVID-19 Chest X-ray Dataset Initiative*” [6] and 2) “*COVID-19 Image Data Collection*” [7]. Pneumonia and Normal cases images are included from the “*Mendeley data 2*” [8]. Figure 2 shows the sample chest X-ray images of COVID-19, Normal and Pneumonia classes from the COVID19CXr dataset.

For the performance assessment of the proposed method, we have used 5-fold cross-validation approach, in which the dataset is divided into 5-folds at the patient level. Table 2 gives details of the distribution of images in the training set, validation set, and test set corresponding to each fold. The training set and

Table 2: Images distribution in the train set, validation set and test set, corresponding to folds

Fold (s)	Data set (s)	COVID-19	Normal	Pneumonia	Total
Fold1	Train Set	189	798	948	1935
	Validation set	25	113	136	274
	Test Set	56	228	271	555
Fold2	Train Set	190	799	951	1940
	Validation set	27	113	135	275
	Test Set	53	227	269	549
Fold3	Train Set	189	798	950	1937
	Validation set	26	113	134	273
	Test Set	55	228	271	554
Fold4	Train Set	193	797	945	1935
	Validation set	27	114	136	277
	Test Set	50	228	274	552
Fold5	Train Set	189	798	952	1939
	Validation set	25	113	136	274
	Test Set	56	228	267	551

validation set are used while training the network, and an hold-out test set is used for the performance assessment of the proposed model.

4.2. Evaluation Metrics

To assess the performance of proposed method we have used sensitivity, specificity, accuracy, positive prediction value (PPV), F1-score, area under the curve (AUC) and confusion matrix as evaluation metrics. The mathematical definition for the evaluation metrics is given below (in Eqn. (5), Eqn. (6), Eqn. (7), Eqn. (8) and Eqn. (9) respectively):

$$Accuracy = \frac{(TP + TN)}{(TP + TN + FP + FN)} \quad (5)$$

$$PPV = \frac{TP}{(TP + FP)} \quad (6)$$

$$Sensitivity = \frac{TP}{(TP + FN)} \quad (7)$$

$$Specificity = \frac{TN}{(TN + FP)} \quad (8)$$

$$F1 - Score = \frac{2TP}{(2TP + FP + FN)} \quad (9)$$

Where true positive (TP), true negative (TN), false positive (FP), and false negative (FN) are the parameters of confusion matrix. The present study deals with a multi-class problem; therefore, to get the overall metric score of the method, we calculated the mean of each metric.

4.3. Results and discussion

In order to evaluate the performance of our proposed stacked convolutional neural network, we conduct a set of experiments. In the first experiment, data augmentation techniques such as flip, rotation, shear, zoom, and shift have been applied on a training set. Thereafter, the augmented training set is utilized for the training of CovNet30 model and fine-tuning VGG19 model. In the second experiment, the stacked CNN model is trained on the validation set. Finally, evaluation results are produced on the test set. We repeat the same

Table 3: Diagnosis performance of stacked CNN model.

Fold (s)	Sensitivity (%)	Specificity (%)	Accuracy (%)	Err \pm CI (%)	PPV (%)	F1-Score	AUC \pm CI
Fold1	95.5	98.19	96.94	3.06 \pm 1.42	97.69	0.97	0.989 \pm 0.003
Fold2	92.66	94.97	91.44	8.56 \pm 2.39	91.32	0.92	0.982 \pm 0.015
Fold3	91.45	95.01	91.34	8.66 \pm 2.35	92.13	0.92	0.982 \pm 0.011
Fold4	92.47	94.77	90.22	9.78 \pm 2.48	85.97	0.88	0.977 \pm 0.023
Fold5	94.59	96.12	93.74	6.26 \pm 2.02	93.54	0.94	0.981 \pm 0.009
Mean	93.33	95.81	92.74	7.26\pm2.16	92.13	0.93	0.984\pm0.012

“Err \pm CI”: classification error (Err) with 95% confidence interval (CI).

“AUC \pm CI”: area under the curve (AUC) with 95% confidence interval (CI).

set of experiments five times for each fold. The following sections represent the experimental results and performance comparison.

4.3.1. *Discrimination power of stacked CNN model:*

Table 3 presents the diagnostic performance of stacked CNN and it shows good discrimination ability for the diagnosis of the COVID-19 from the chest

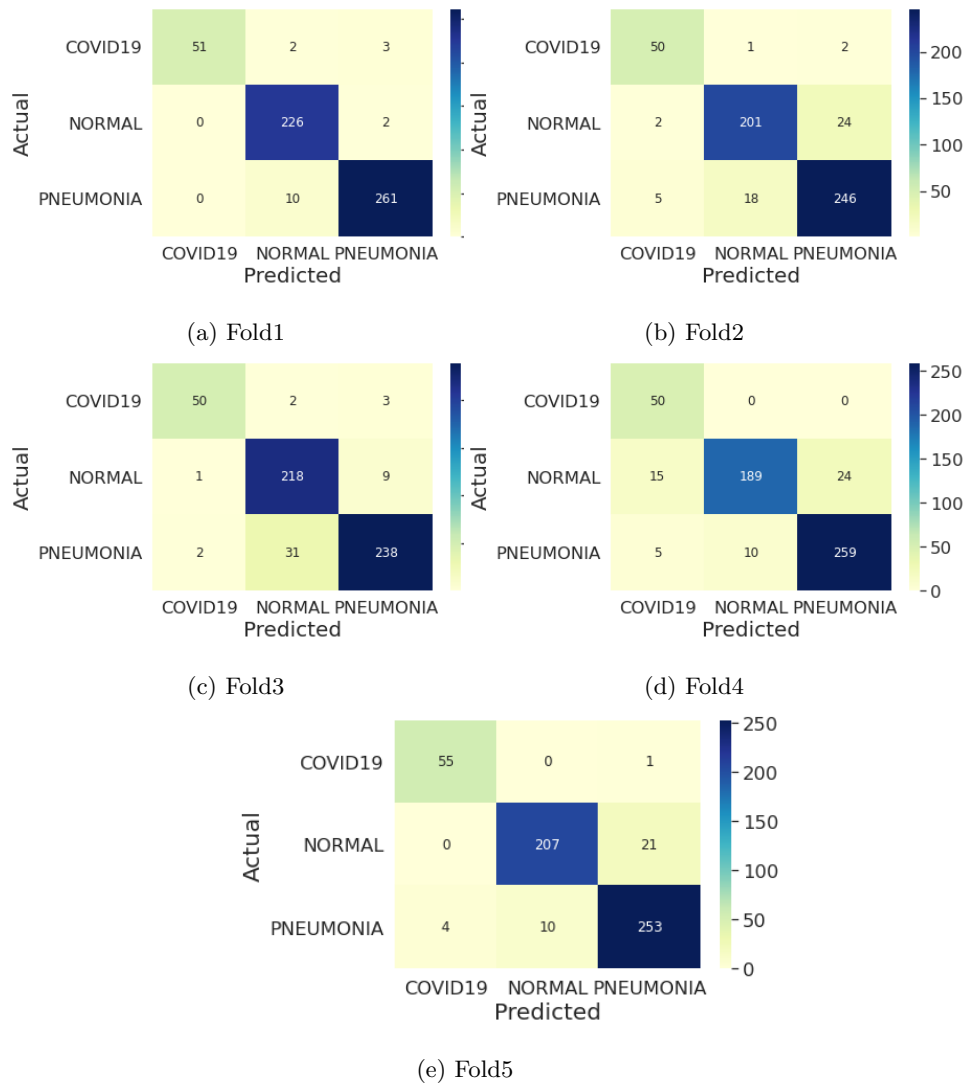


Figure 3: Confusion matrix for stacked CNN model on the different folds.

X-ray images. The proposed model achieved mean sensitivity of 93.33 %, specificity of 95.81 %, PPV of 92.74 %, and accuracy of 92.74 % to classify: COVID-19, Normal and Pneumonia classes. Our method achieved good sensitivity; so that we can limit the miss classification of the COVID-19 positive cases. In ad-

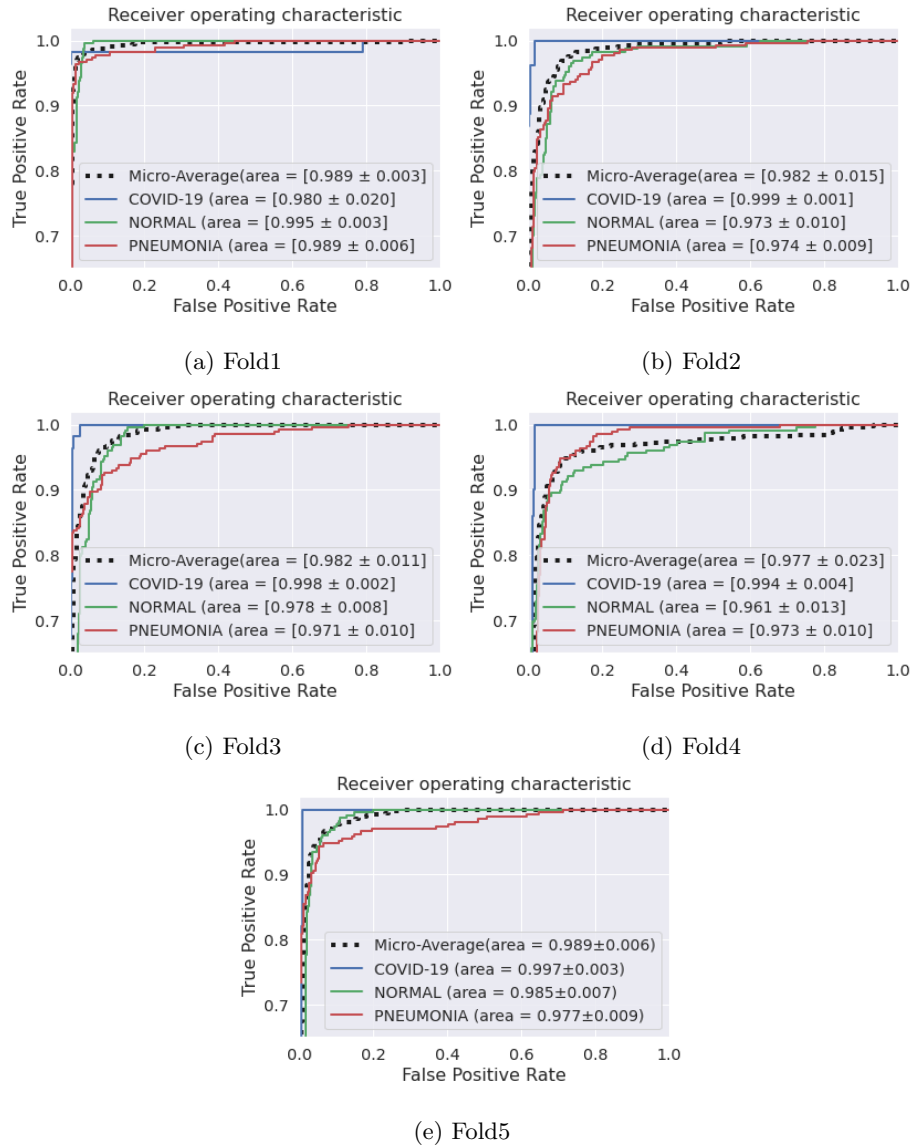


Figure 4: ROC curve for stacked CNN model on the different folds.

dition, the confidence interval for the classification error and AUC is calculated at the 95% confidence level. As shown in Table 3 the classification error of the proposed model is $7.26\% \pm 2.16\%$ at the 95% confidence level.

For a deeper exploration of the performances of the proposed method the confusion matrix and receiver operating characteristic (ROC) curve (with AUC's CI) corresponding to each fold are evaluated and shown in Figure 3 and Figure 4, respectively. It can be observed from the confusion matrix the proposed model produce very less false negative and false positive, specifically for the COVID-19 cases compared to other cases of COVID19CXr dataset. For COVID-19 cases, it is essential to minimize the wrong diagnosis. On the other hand, the ROC curve shows the stability of the proposed stacked CNN model, and the present model achieved a mean AUC of 0.994 for COVID-19 class and a mean AUC of 0.984 along with CI of [0.012]for all categories.

4.3.2. Performance comparison:

Table 4 shows the performance comparison of the proposed method, VGG19 and CovNet30. It is observed from Table 4 that the proposed model achieves the best accuracy of 92.74 % compared to stand-alone model VGG19 and CovNet30, our stacked CNN model improves the diagnosis accuracy by 2.88% ~ 5.01%. In terms of sensitivity, specificity, and PPV, proposed model also shows sig-

Table 4: Performance comparison for different methods.

Metric	Method		
	VGG19	CovNet30	Proposed
Accuracy (%)	89.86±2.21	87.73±3.08	92.74±2.68
Sensitivity (%)	90.34±4.24	86.80±4.05	93.33±1.66
Specificity (%)	94.15±1.26	93.49±1.39	95.81±1.43
PPV (%)	90.53±2.96	84.54±5.23	92.13±4.23
F1-score	0.90±0.03	0.85±0.04	0.93±0.03
AUC	0.97±0.01	0.97±0.02	0.98±0.01

Table 5: Performance evaluation of the sub-models.

Model (s)		Fold1	Fold2	Fold3	Fold4	Fold5
CovNet30	Sub-model1	86.3	89.4	51.6	59.1	84
	Sub-model2	95.7	91.1	86.5	83.5	90.4
	Sub-model3	85.4	84.9	89.4	85.9	57.5
VGG19	Sub-model4	93.3	87.8	79.6	90.2	79.9
	Sub-model5	92.8	89.4	87.9	90.4	91.1
Proposed model		96.94	91.44	91.34	90.22	93.54

nificant performance improvements by 2.99% \sim 6.53%, 1.66% \sim 2.32%, and 1.6% \sim 7.59%, respectively. Further, Table 5 represents the performance of the individual sub-models and the proposed stacked CNN model corresponding to each fold. Our stacked ensemble CNN model achieved better performance as compared to all sub-models, over the each fold.

A variety of deep learning-based studies have already been proposed in past studies for COVID-19 diagnosis from the chest X-ray images. The performance comparison of the proposed method in the present study with some of related studies are shown in the Table 6.

Since COVID-19 is a new epidemic and there are limited number of COVID-19 X-ray images are available publicly for developing CAD systems for COVID-19 detection. Studies in [26] and [17] have just developed on the 25 and 50 images for each class, respectively. Other studies in the [18, 19, 20, 21, 24] have used less 200 COVID-19 images for developing their methods. In this study, a total of 2764 X-ray images has been used to develop our model, including 270 COVID-19 images, which the largest number of COVID-19 images among all the studies in Table 6. It can be observed from Table 6 that for the multi-class classification task, the proposed approach shows the superiority over the methods in [18, 19, 20, 21], except the method in [24], which has higher accuracy. However, sensitivity is higher for our approach.

Some of the salient features of stacked CNN can be summarized as:

Table 6: Performance comparison with existing methods

Author (s)	Method	Dataset		Classification Task	Results
		Modality	Subjects		
Narin et al. [17]	Pre-Train CNN	X-ray	50 COVID-19, 50 Normal	Binary: COVID-19, Normal	97 % (Acc)
Wang et al. [18]	COVID-Net	X-ray	183 COVID-19, 8066 Normal, 5538 non-COVID19	Multiclass: COVID-19, Normal, Non-COVID19	92.6% (Acc)
Oh et al. [19]	ResNet18	X-ray	191 Normal, 54 Bacterial, 57 Tuberculosis, 20 Viral, 180 COVID-19	Multiclass: Normal, Bacterial, Tuberculosis, Viral, COVID-19	88.9% (Acc)
Ozturk et al. [20]	DarkCovidNet	X-ray	127 COVID-19, 500 no-findings, 500 pneumonia	Binary: COVID-19, No-findings Multiclass: COVID-19, No-findings, Pneumonia	98.08% (Acc) 87.02% (Acc)
Pereira et al. [21]	Deep features, Texture features, Fusion techniques	X-ray	200 Normal, 180 COVID-19, 22 SARS, 20 MERS, 22 Pneumocystis, 24 Streptococcus, 20 Varicella	Hierarchical: Normal, COVID-19, SARS, MERS, Pneumocystis, Streptococcus, Varicella	0.89 (F1-score)
Ucar et al. [24]	SqueezeNet CNN	X-ray	1583 Normal, 4290 Pneumonia, 76 COVID-19	Multiclass: Normal, Pneumonia, COVID-19	95.7 % (Acc), 90 % (Sens)
Sethy et al. [26]	Deep feature, SVM	X-ray	25 COVID-19+, 25 COVID-19-	Binary: COVID-19+, COVID-19-	95.38% (Acc)
Proposed Method	Stacked CNN	X-ray	270 COVID-19, 1139 Normal, 1355 Pneumonia	Multiclass: COVID-19, Normal, Pneumonia	92.74% (Acc) 93.33 % (Sens) 0.93 (F1-Score)

- The proposed method is based on the stacked generalization of CNN's sub-models, which minimizes the variance of predictions and reduces generalization error. As of the result, stacked CNN yields high diagnosis accuracy in the X-ray images.
- The proposed stacked CNN model produces very less false positive (type 1) and false negative (type 2) error, which confirms that the stacked CNN is reliable for clinical uses.
- The proposed model is developed based on a less complex network, which

computationally efficient and shows its stability on a small dataset.

5. CONCLUSION

In this paper, we introduced a new stacked convolutional neural network for the automatic diagnosis of the COVID19 from the Chest X-ray images. In the proposed method, CNN's sub-models have obtained from our developed CovNet30 model and pre-trained VGG19 model. Stacked CNN model ensemble the sub-models using logistic regression, for deriving a powerful model for image classification than individual sub-models. The proposed model is able to learn image discriminative features and retrieved the diverse information present in the X-ray images of the chest. It achieves a classification accuracy of 92.74%, sensitivity of 93.33%, PPV of 92.13%, and F1-score of 0.93 on the chest X-ray images of COVID19CXr dataset. Our proposed approach shows its superiority over the existing methods for the diagnosis of the COVID-19 from the X-ray images.

Our experiments results show the effectiveness of the stacked CNN for classification of COVID-19, Normal, and Pneumonia X-ray images. More importantly, the proposed model outperforms the pre-trained VGG19 and CovNet30 model for the classification of X-ray images.

References

- [1] H. Nishiura, N. M. Linton, A. R. Akhmetzhanov, Serial interval of novel coronavirus (covid-19) infections, *International journal of infectious diseases* (2020).
- [2] Y. Chen, Q. Liu, D. Guo, Emerging coronaviruses: genome structure, replication, and pathogenesis, *Journal of medical virology* 92 (4) (2020) 418–423.
- [3] W. H. Organization, et al., Novel coronavirus (2019-ncov) technical guidance: laboratory testing for 2019-ncov in humans, World Health Organization, Geneva, Switzerland. <https://www.who.int/publications/i/item/9789241502615>.

who. [int/emergencies/diseases/novel-coronavirus-2019/technical-guidance/laboratory-guidance](https://www.who.int/emergencies/diseases/novel-coronavirus-2019/technical-guidance/laboratory-guidance) (2020).

- [4] M.-Y. Ng, E. Y. Lee, J. Yang, F. Yang, X. Li, H. Wang, M. M.-s. Lui, C. S.-Y. Lo, B. Leung, P.-L. Khong, et al., Imaging profile of the covid-19 infection: radiologic findings and literature review, *Radiology: Cardiothoracic Imaging* 2 (1) (2020) e200034.
- [5] C. Huang, Y. Wang, X. Li, L. Ren, J. Zhao, Y. Hu, L. Zhang, G. Fan, J. Xu, X. Gu, et al., Clinical features of patients infected with 2019 novel coronavirus in wuhan, china, *The lancet* 395 (10223) (2020) 497–506.
- [6] C. et al., Figure 1 covid-19 chest x-ray data initiative. (2020).
URL <https://github.com/agchung/Figure1-COVID-chestxraydataset>
- [7] J. P. Cohen, P. Morrison, L. Dao, Covid-19 image data collection, arXiv preprint arXiv:2003.11597 (2020).
URL <https://github.com/ieee8023/covid-chestxray-dataset>
- [8] D. Kermany, K. Zhang, M. Goldbaum, Labeled optical coherence tomography (oct) and chest x-ray images for classification, *Mendeley data* 2 (2018).
- [9] K. Doi, Computer-aided diagnosis in medical imaging: historical review, current status and future potential, *Computerized medical imaging and graphics* 31 (4-5) (2007) 198–211.
- [10] G. Castellano, L. Bonilha, L. Li, F. Cendes, Texture analysis of medical images, *Clinical radiology* 59 (12) (2004) 1061–1069.
- [11] B. Van Ginneken, S. Katsuragawa, B. M. ter Haar Romeny, K. Doi, M. A. Viergeever, Automatic detection of abnormalities in chest radiographs using local texture analysis, *IEEE transactions on medical imaging* 21 (2) (2002) 139–149.
- [12] S. Jaeger, A. Karargyris, S. Candemir, L. Folio, J. Siegelman, F. Callaghan, Z. Xue, K. Palaniappan, R. K. Singh, S. Antani, et al., Automatic tuber-

culosis screening using chest radiographs, *IEEE transactions on medical imaging* 33 (2) (2013) 233–245.

- [13] F. Shi, J. Wang, J. Shi, Z. Wu, Q. Wang, Z. Tang, K. He, Y. Shi, D. Shen, Review of artificial intelligence techniques in imaging data acquisition, segmentation and diagnosis for covid-19, *IEEE Reviews in Biomedical Engineering* (2020).
- [14] D. Dong, Z. Tang, S. Wang, H. Hui, L. Gong, Y. Lu, Z. Xue, H. Liao, F. Chen, F. Yang, et al., The role of imaging in the detection and management of covid-19: a review, *IEEE Reviews in Biomedical Engineering* (2020).
- [15] C. Butt, J. Gill, D. Chun, B. A. Babu, Deep learning system to screen coronavirus disease 2019 pneumonia, *Applied Intelligence* (2020) 1.
- [16] A. A. Ardakani, A. R. Kanafi, U. R. Acharya, N. Khadem, A. Mohammadi, Application of deep learning technique to manage covid-19 in routine clinical practice using ct images: Results of 10 convolutional neural networks, *Computers in Biology and Medicine* (2020) 103795.
- [17] A. Narin, C. Kaya, Z. Pamuk, Automatic detection of coronavirus disease (covid-19) using x-ray images and deep convolutional neural networks, *arXiv preprint arXiv:2003.10849* (2020).
- [18] L. Wang, A. Wong, Covid-net: A tailored deep convolutional neural network design for detection of covid-19 cases from chest radiography images, *arXiv preprint arXiv:2003.09871* (2020).
- [19] Y. Oh, S. Park, J. C. Ye, Deep learning covid-19 features on cxr using limited training data sets, *IEEE Transactions on Medical Imaging* (2020).
- [20] T. Ozturk, M. Talo, E. A. Yildirim, U. B. Baloglu, O. Yildirim, U. R. Acharya, Automated detection of covid-19 cases using deep neural networks with x-ray images, *Computers in Biology and Medicine* (2020) 103792.

- [21] R. M. Pereira, D. Bertolini, L. O. Teixeira, C. N. Silla Jr, Y. M. Costa, Covid-19 identification in chest x-ray images on flat and hierarchical classification scenarios, *Computer Methods and Programs in Biomedicine* (2020) 105532.
- [22] J. Wang, Y. Bao, Y. Wen, H. Lu, H. Luo, Y. Xiang, X. Li, C. Liu, D. Qian, Prior-attention residual learning for more discriminative covid-19 screening in ct images, *IEEE Transactions on Medical Imaging* (2020).
- [23] S. Hu, Y. Gao, Z. Niu, Y. Jiang, L. Li, X. Xiao, M. Wang, E. F. Fang, W. Menpes-Smith, J. Xia, et al., Weakly supervised deep learning for covid-19 infection detection and classification from ct images, *arXiv preprint arXiv:2004.06689* (2020).
- [24] F. Ucar, D. Korkmaz, Covidiagnosis-net: Deep bayes-squeezenet based diagnostic of the coronavirus disease 2019 (covid-19) from x-ray images, *Medical Hypotheses* (2020) 109761.
- [25] P. Afshar, S. Heidarian, F. Naderkhani, A. Oikonomou, K. N. Plataniotis, A. Mohammadi, Covid-caps: A capsule network-based framework for identification of covid-19 cases from x-ray images, *arXiv preprint arXiv:2004.02696* (2020).
- [26] P. K. Sethy, S. K. Behera, Detection of coronavirus disease (covid-19) based on deep features, *Preprints 2020030300* (2020) 2020.
- [27] A. Krizhevsky, I. Sutskever, G. E. Hinton, Imagenet classification with deep convolutional neural networks, in: *Advances in neural information processing systems*, 2012, pp. 1097–1105.
- [28] K. He, X. Zhang, S. Ren, J. Sun, Deep residual learning for image recognition, in: *Proceedings of the IEEE conference on computer vision and pattern recognition*, 2016, pp. 770–778.
- [29] K. Simonyan, A. Zisserman, Very deep convolutional networks for large-scale image recognition, *arXiv preprint arXiv:1409.1556* (2014).

- [30] R. Girshick, J. Donahue, T. Darrell, J. Malik, Rich feature hierarchies for accurate object detection and semantic segmentation, in: Proceedings of the IEEE conference on computer vision and pattern recognition, 2014, pp. 580–587.
- [31] R. Girshick, Fast r-cnn, in: Proceedings of the IEEE international conference on computer vision, 2015, pp. 1440–1448.
- [32] M. Gour, S. Jain, R. Agrawal, Deeprnnnetseg: Deep residual neural network for nuclei segmentation on breast cancer histopathological images, in: International Conference on Computer Vision and Image Processing, Springer, 2019, pp. 243–253.
- [33] O. Ronneberger, P. Fischer, T. Brox, U-net: Convolutional networks for biomedical image segmentation, in: International Conference on Medical image computing and computer-assisted intervention, Springer, 2015, pp. 234–241.
- [34] M. Gour, S. Jain, T. S. Kumar, Residual learning based cnn for breast cancer histopathological image classification, International Journal of Imaging Systems and Technology (2020).
- [35] S. M. Anwar, M. Majid, A. Qayyum, M. Awais, M. Alnowami, M. K. Khan, Medical image analysis using convolutional neural networks: a review, Journal of medical systems 42 (11) (2018) 226.
- [36] D. Shen, G. Wu, H.-I. Suk, Deep learning in medical image analysis, Annual review of biomedical engineering 19 (2017) 221–248.
- [37] X. Huang, J. Shan, V. Vaidya, Lung nodule detection in ct using 3d convolutional neural networks, in: 2017 IEEE 14th International Symposium on Biomedical Imaging (ISBI 2017), IEEE, 2017, pp. 379–383.
- [38] P. Rajpurkar, J. Irvin, K. Zhu, B. Yang, H. Mehta, T. Duan, D. Ding, A. Bagul, C. Langlotz, K. Shpanskaya, et al., Chexnet: Radiologist-level

pneumonia detection on chest x-rays with deep learning, arXiv preprint arXiv:1711.05225 (2017).

- [39] C. Liu, Y. Cao, M. Alcantara, B. Liu, M. Brunette, J. Peinado, W. Curioso, Tx-cnn: Detecting tuberculosis in chest x-ray images using convolutional neural network, in: 2017 IEEE International Conference on Image Processing (ICIP), IEEE, 2017, pp. 2314–2318.
- [40] L. Breiman, Stacked regressions, *Machine learning* 24 (1) (1996) 49–64.
- [41] D. P. Kingma, J. Ba, Adam: A method for stochastic optimization, arXiv preprint arXiv:1412.6980 (2014).
- [42] D. H. Wolpert, Stacked generalization, *Neural networks* 5 (2) (1992) 241–259.
- [43] F. Pedregosa, G. Varoquaux, A. Gramfort, V. Michel, B. Thirion, O. Grisel, M. Blondel, P. Prettenhofer, R. Weiss, V. Dubourg, J. Vanderplas, A. Passos, D. Cournapeau, M. Brucher, M. Perrot, E. Duchesnay, Scikit-learn: Machine learning in Python, *Journal of Machine Learning Research* 12 (2011) 2825–2830.
URL <https://scikit-learn.org/stable/modules/generated/sklearn.multiclass.OneVsRestClassifier.html>